

LISA Pathfinder最初の結果

道村唯太

東京大学 大学院理学系研究科 物理学専攻

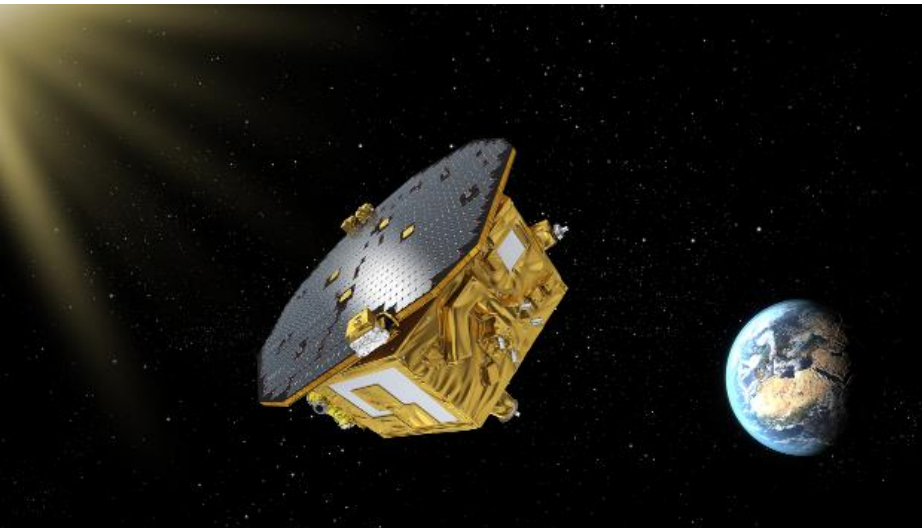
LISA Pathfinder

- 宇宙重力波望遠鏡LISAの技術実証機
LISA: Laser Interferometer Space Antenna
- 2015年12月3日 打ち上げ成功
- 2016年1月22日 L1に到達
- 2016年2月22日 ドラッグフリー達成
- 2016年3月1日 science mission開始
- 2016年6月7日 最初の結果公開



<http://spaceflight101.com/lisa-pathfinder/photos-vega-lights-up-the-night-over-the-amazon-launching-lisa-pathfinder/>

<http://sci.esa.int/lisa-pathfinder/56910-lisa-pathfinder-in-space/>



esa

公開された論文

- M. Armano+, [PRL 116, 231101 \(2016\)](#)
Sub-Femto-g Free Fall for Space-Based Gravitational Wave Observatories: LISA Pathfinder Results
- 加速度雑音と変位雑音を評価
→LISAが可能

PRL 116, 231101 (2016)  Selected for a Viewpoint in *Physics* week ending 10 JUNE 2016
PHYSICAL REVIEW LETTERS



Sub-Femto-g Free Fall for Space-Based Gravitational Wave Observatories: LISA Pathfinder Results

M. Armano,¹ H. Audley,² G. Auger,³ J. T. Baird,⁴ M. Bassan,⁵ P. Binetruy,³ M. Born,² D. Bortoluzzi,⁶ N. Brandt,⁷ M. Caleno,⁸ L. Carbone,⁹ A. Cavalleri,¹⁰ A. Cesarini,⁹ G. Ciani,^{9,†} G. Congedo,^{9,‡} A. M. Cruise,¹¹ K. Danzmann,² M. de Deus Silva,¹ R. De Rosa,¹² M. Diaz-Aguiló,¹³ L. Di Fiore,¹⁴ I. Diepholz,² G. Dixon,¹¹ R. Dolesi,⁹ N. Dunbar,¹⁵ L. Ferraioli,¹⁶ V. Ferroni,⁹ W. Fichter,¹⁷ E. D. Fitzsimons,¹⁸ R. Flatscher,⁷ M. Freschi,¹ A. F. García Marín,^{2,§} C. García Marirrodriga,⁸ R. Gerndt,⁷ L. Gesa,¹³ F. Gibert,⁹ D. Giardini,¹⁶ R. Giusteri,⁹ F. Guzmán,^{2,||} A. Grado,¹⁹ C. Grimani,²⁰ A. Grynagier,^{17,¶} J. Grzysimisch,⁸ I. Harrison,²¹ G. Heinzel,² M. Hewitson,² D. Hollington,⁴ D. Hoyland,¹¹ M. Hueller,⁹ H. Inchauspé,³ O. Jennrich,⁸ P. Jetzer,²² U. Johann,⁷ B. Johlander,⁸ N. Kamesis,² B. Kaune,² N. Korsakova,² C. J. Killow,²³ J. A. Lobo,^{13,*} I. Lloro,¹³ L. Liu,⁹ J. P. López-Zaragoza,¹³ R. Maarschalkerweerd,²¹ D. Mance,¹⁶ V. Martín,¹³ L. Martin-Polo,¹ J. Martino,³ F. Martin-Porqueras,¹ S. Madden,⁸ I. Mateos,¹³ P. W. McNamara,⁸ J. Mendes,²¹ L. Mendes,¹ A. Monsky,^{2,§} D. Nicolodi,^{9,**} M. Nofrarias,¹³ S. Paczkowski,² M. Perreux-Lloyd,²³ A. Petiteau,⁸ P. Pivato,⁹ E. Plagnol,³ P. Prat,³ U. Ragnit,⁸ B. Raïs,³ J. Ramos-Castro,²⁴ J. Reiche,² D. I. Robertson,²³ H. Rozemeijer,⁸ F. Rivas,¹³ G. Russano,⁹ J. Sanjuán,^{13,††} P. Sarra,²⁵ A. Schleicher,⁷ D. Shaul,⁴ J. Slutsky,²⁶ C. F. Sopena,¹³ R. Stanga,²⁷ F. Steier,^{2,§§} T. Sumner,⁴ D. Texier,¹ J. I. Thorpe,²⁶ C. Trenkel,¹⁵ M. Tröbs,² H. B. Tu,^{9,‡‡} D. Vetrugno,⁹ S. Vitale,⁹ V. Wand,^{2,§§} G. Wanner,² H. Ward,²³ C. Warren,¹⁵ P. J. Wass,⁴ D. Wealthy,¹⁵ W. J. Weber,⁹ L. Wissel,² A. Wittchen,² A. Zambotti,⁶ C. Zanoni,⁶ T. Ziegler,⁷ and P. Zweifel¹⁶

¹European Space Astronomy Centre, European Space Agency, Villanueva de la Cañada, 28692 Madrid, Spain

²Albert-Einstein-Institut, Max-Planck-Institut für Gravitationsphysik und Leibniz Universität Hannover, Callinstraße 38, 30167 Hannover, Germany

PHYSICAL REVIEW LETTERS

Highlights Recent Accepted Collections Authors R

Featured in Physics

Editors' Suggestion

Open Access

Sub-Femto-*g* Free Fall for Space-Based Gravitational Wave Observatories: LISA Pathfinder Results

M. Armano *et al.*

Phys. Rev. Lett. **116**, 231101 – Published 7 June 2016

Physics See Viewpoint: [Paving the Way to Space-Based Gravitational-Wave Detectors](#)



得られた雑音スペクトル

- $(5.2 \pm 0.1) \text{ fm s}^{-2}/\sqrt{\text{rtHz}}$ $(34.8 \pm 0.3) \text{ fm}/\sqrt{\text{rtHz}}$

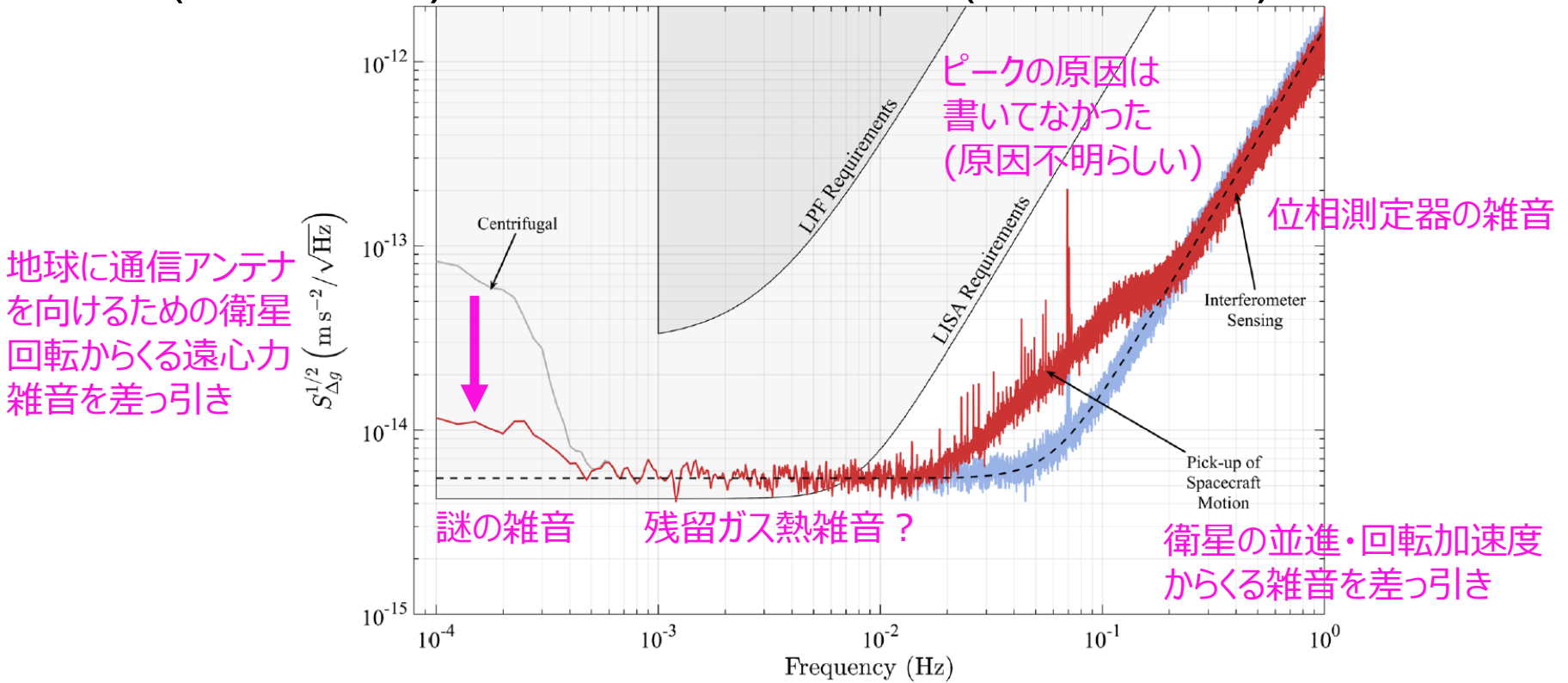


FIG. 1. Gray: ASD of Δg , $S_{\Delta g}^{1/2}(f)$, measured for 6.5 days starting 127 days after launch. The ASD is the result of averaging 26 periodograms of 40 000 s each, which results in a relative error (1σ) of 10% in $S_{\Delta g}^{1/2}$. The effective spectral resolution, set by the spectral window, is $\Delta f \approx \pm 50 \mu\text{Hz}$. The absolute calibration of the measurement is better than 5%. Red: ASD of the same time series after correction for the centrifugal force (visible at the lowest frequencies). Light blue: ASD after correction for the pickup of spacecraft motion by the interferometer (IFO), visible in the 20–200 mHz range. Dashed smooth black line: $S_{\Delta g}(f) = S_0 + S_{\text{IFO}}(2\pi f)^4$ with $S_0^{1/2} = (5.57 \pm 0.04) \text{ fm s}^{-2}/\sqrt{\text{Hz}}$ and $S_{\text{IFO}}^{1/2} = (34.8 \pm 0.3) \text{ fm}/\sqrt{\text{Hz}}$. Note that the level of S_0 has decreased further in subsequent measurements, as quoted in the abstract and shown in Fig. 3. Shaded areas: LISA and LISA Pathfinder requirements for Δg . The LISA single test-mass acceleration requirement [2] has been multiplied by $\sqrt{2}$ to be presented here as a differential acceleration. 4

残留ガス熱雑音か？

- 9.5 μPa の H_2O で説明可能
(H_2 なら3倍)
- 加速度雑音レベルは1/tで
次第に減少
- 2月始めに宇宙に開放して
真空引きを始めたばかり
- 温度変調して $dF/d\Delta T$ を測定
することにより $< 22 \mu\text{Pa}$
であることは別途測定した

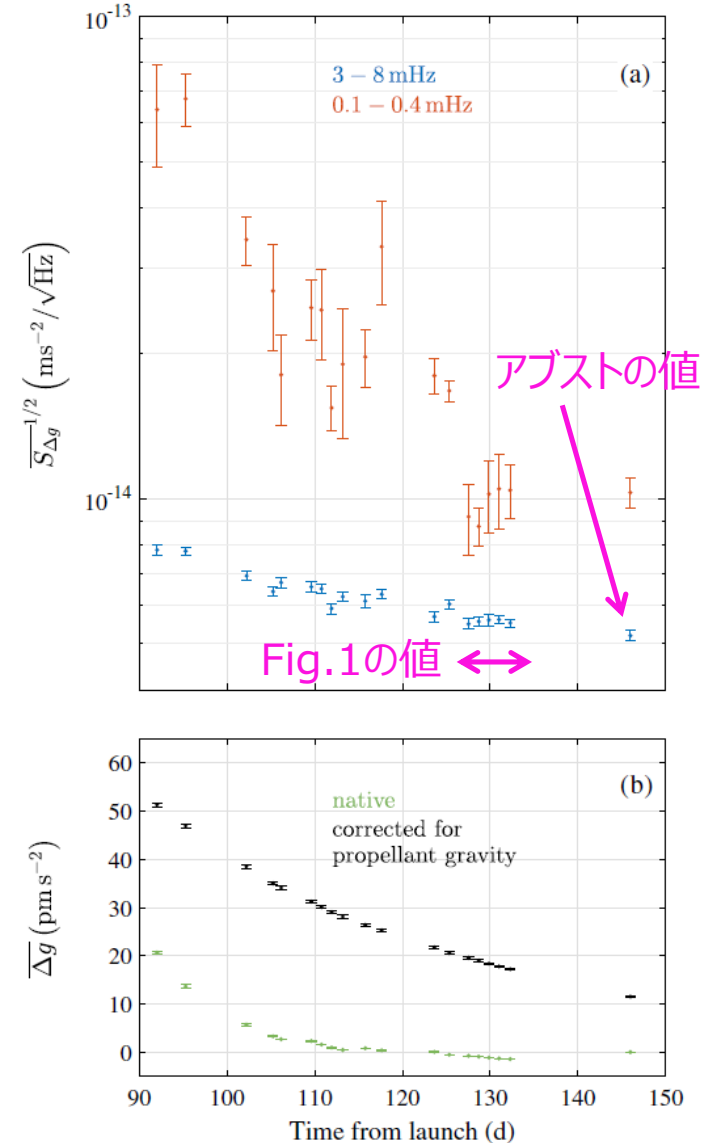


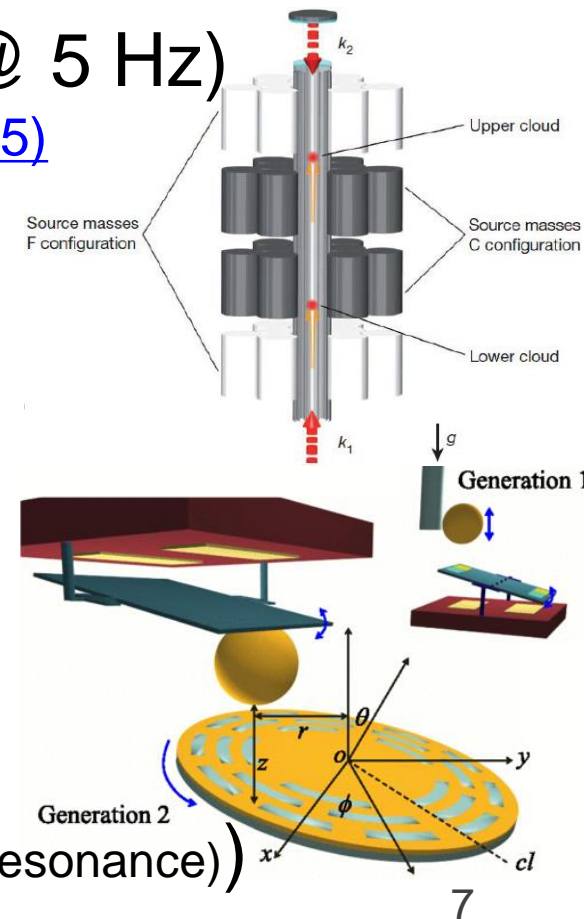
FIG. 3. (a) Square root of the averaged power spectral density of Δg in the 3–8 mHz and 0.1–0.4 mHz frequency bands of the time of flight. This is plotted for comparison with the noise level of the accelerometer. (b) Δg versus time from launch. The 'native' data is the raw data, and the 'corrected for propellant gravity' data is the data after correction for the gravity of the propellant. The 'Abstr. value' is the value of the 'Abstr.' data point at approximately 145 days.

0.5 mHz以下の謎の雑音

- アクチュエータ雑音 → ×
DC的な相対加速度は予想よりも小さかった(し次第に減少している)のでforce authority(制御ゲイン?)を下げたため、当初の想定よりも効いていない
- 帯電変動 → たぶん違う($\sim 3 \text{ fm s}^{-2}/\text{rtHz}$ @ 0.1 mHz)
今後わざと帯電させて測定する予定
- 熱勾配雑音 → $< \sim 1 \text{ fm s}^{-2}/\text{rtHz}$ @ 0.1 mHz
 $50 \text{ } \mu\text{K}/\text{rtHz}$ @ 0.1 mHz (サーミスタ)
- 古典輻射圧雑音 → $\sim 2 \text{ fm s}^{-2}/\text{rtHz}$
 $0.4 \text{ } \mu\text{W}/\text{rtHz}$
- 磁場雑音 → $< \sim 3 \text{ fm s}^{-2}/\text{rtHz}$ @ 0.1 mHz
 $100 \text{ nT}/\text{rtHz}$ @ 0.1 mHz (磁場センサ)
- 時間とともに減少しているのも謎(推進薬の減少と関係?)

どのくらいすごいのか？

- 重力波検出器として
 - $h \sim 9.3e-14$ /rtHz @ 0.1 Hz
(腕長: 376 mm)
(cf. Phase-II TOBA: $1e-10$ /rtHz @ 5 Hz)
[A. Shoda PhD thesis \(University of Tokyo, 2015\)](#)
- 万有引力定数Gの測定
 - $0.54e-15 * g$ /rtHz @ 0.7-20 mHz
(c.f 原子干渉計: $3e-9 * g$ @ 1sec)
G. Rosi+, [Nature 510, 518 \(2014\)](#)
- 重力逆二乗則の検証
 - 10 fN/rtHz @ 0.7-20 mHz
(TM: 1.928 kg)
(cf. MTO: 6 fN/rtHz @ 307 Hz (on resonance))
Y.-J. Chen+, [PRL 116, 221102 \(2016\)](#)



その他衛星との比較



- 加速度雑音

https://en.wikipedia.org/wiki/Gravity_Recovery_and_Climate_Experiment

LPF: $5.2 \times 10^{-15} \text{ m s}^{-2}/\text{rtHz}$ @ 0.7-20 mHz (1.928 kg)

GRACE: $1 \times 10^{-10} \text{ m s}^{-2}/\text{rtHz}$ @ 1 mHz (< 100 g)

GOCE: $3 \times 10^{-12} \text{ m s}^{-2}/\text{rtHz}$ @ 1 mHz (320 g)

Pre-DECIGO要求値: $3 \times 10^{-18} \text{ m s}^{-2}/\text{rtHz}$ (30 kg)

- 変位雑音

LPF: $3.48 \times 10^{-14} \text{ m}/\text{rtHz}$ @ 0.1 Hz

Pre-DECIGO要求値: $2 \times 10^{-18} \text{ m}/\text{rtHz}$ @ 0.1 Hz

http://www.esa.int/Our_Activities/Observing_the_Earth/GOCE/Introducing_GOCE

LPFは地球から $1.5 \times 10^6 \text{ km}$ 離れた
ラグランジュ点L1でのリサーチ軌道
GRACE, GOCEは地球周回軌道で
高度350 km, 250 km
Pre-DECIGOは未定(地球周回?)

LPF, GOCE, Pre-DECIGOはドラッグフリー

http://www.rssd.esa.int/SP/LISAPATHFINDER/doc/LPF_Science_Case.pdf



GOCE

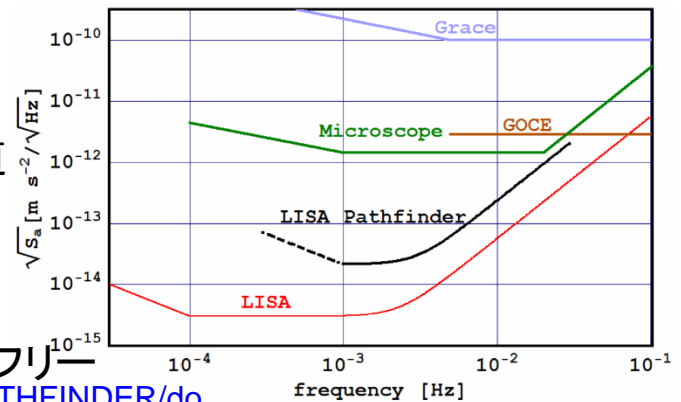


Figure 5: Comparison of required performances of various missions for relative geosismic deviation of test-mass pairs. For LISA Pathfinder the mission requirements are reported as the solid line. The dashed tail is a design goal. Actual projected performance is discussed later.

較正とか

- 不確かさは5 %以下らしい
 - 較正ラインで地上試験との一致を 2σ で確認
 - レーザー強度を変調させ、輻射圧で独立に較正して20 %の精度で一致を確認
 - 論文中、eLISAの名前は一度も出ていない
 - GW150914のことは一切触れられてない
 - LPF単体での科学的成果についても触れられてない
- Vitale, however, points out that it is important for researchers to stay focused on the mission's immediate goal. *“Our main objective is to demonstrate freefall,”* he says, *“and we don’t want to be distracted from that.”*

<http://www.nature.com/news/freefall-space-cubes-are-test-for-gravitational-wave-spotter-1.18806>

測定方法

- ヘテロダイン干渉計
(35 mW @ 1064 nm)
- 衛星に対するTM1の動き
がなくなるように
 μN スラスタで衛星を
ドラッグフリー制御
- TM1に対するTM2動き
がなくなるようにTM2
の動きを静電アクチュ
エータで制御
- 4つの干渉計
reference, frequency,
X1, X12

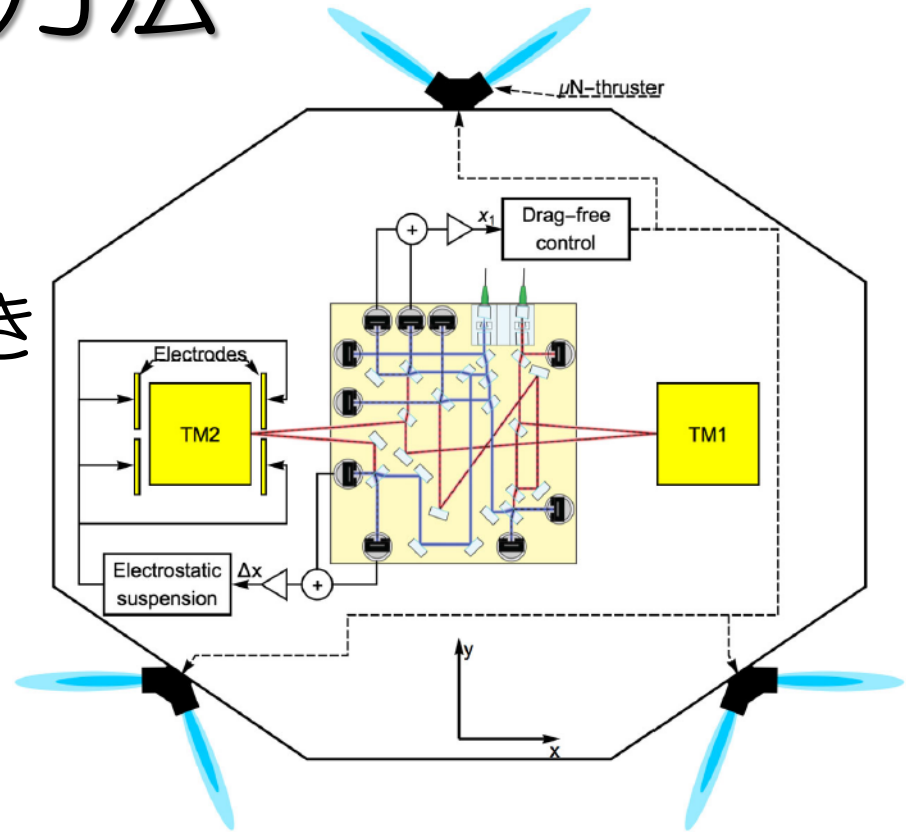
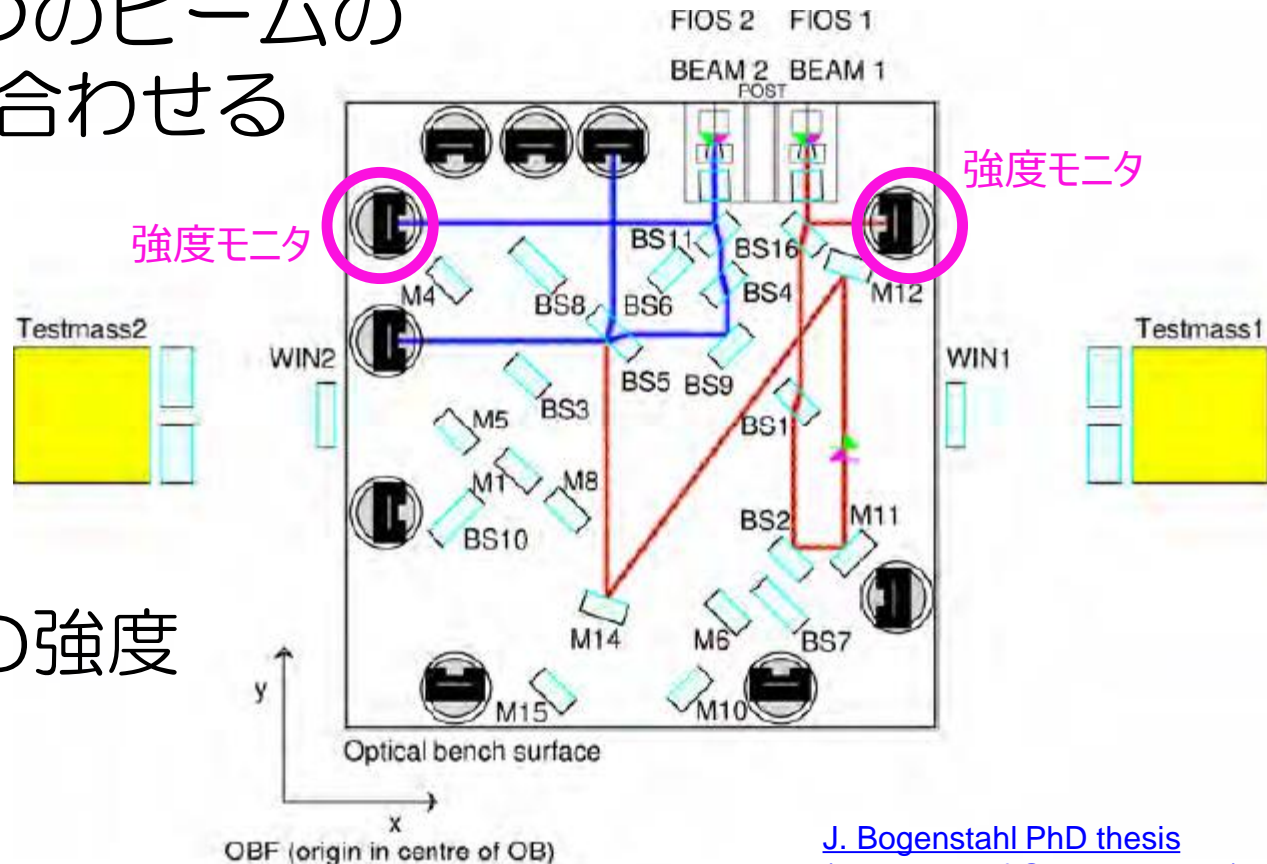


FIG. 2. A schematic of LPF. The figure shows TM1, TM2, and the optical bench beam paths for measuring Δx and x_1 . The measurement of Δx drives the electrostatic suspension of TM2, which applies the necessary electrostatic forces by means of the electrodes represented by the four gold plates facing TM2. All other electrodes surrounding the TMs are not shown. The measurement of x_1 drives the drag-free control loop that uses the micronewton thrusters to exert forces on the spacecraft. The figure depicts the x and y axes we use in this Letter, while z is normal to the figure.

参照干渉計

- 2つのビームの相対位相を測定
ファイバで導入される位相差など
制御して2つのビームの
相対位相を合わせる

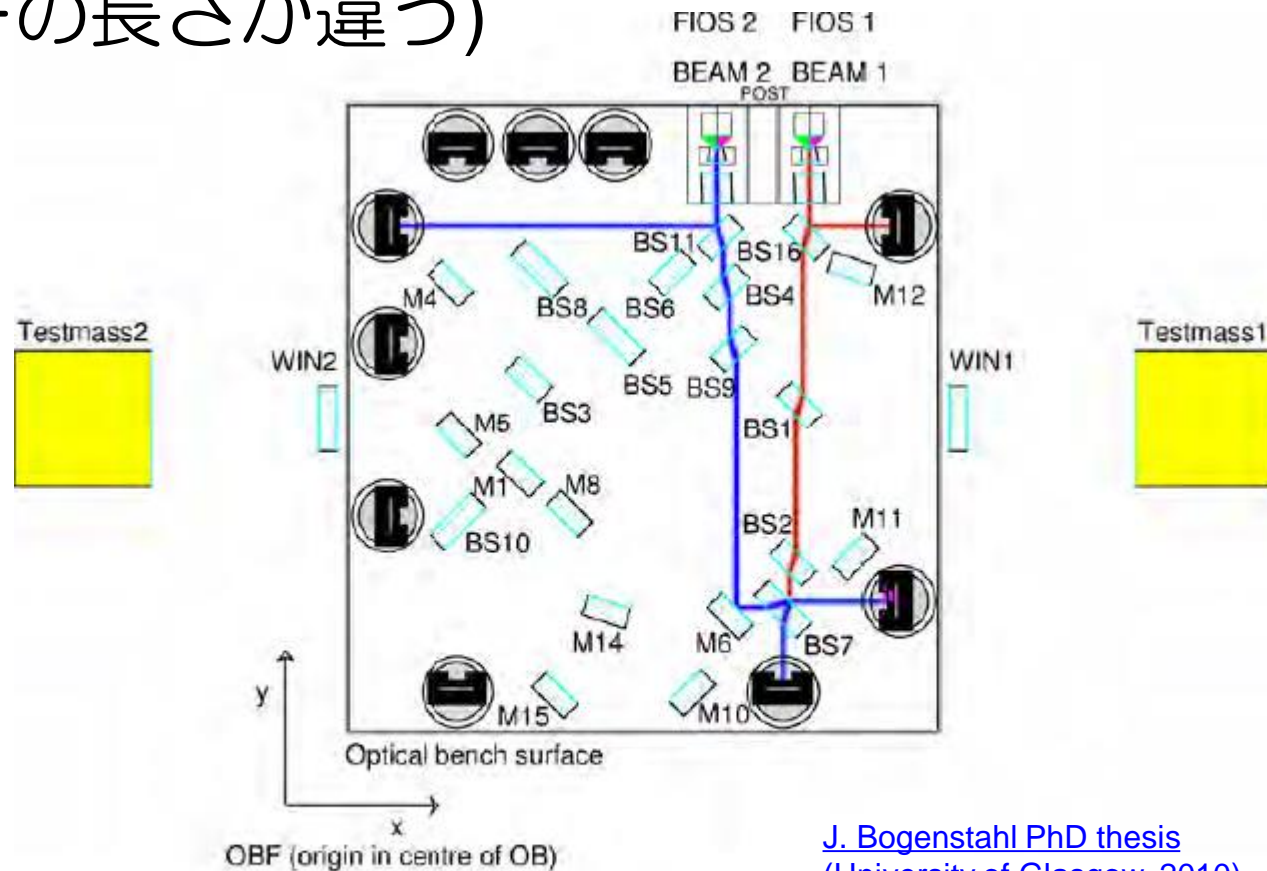


- 2つのビームの強度
モニタもある

[J. Bogenstahl PhD thesis
\(University of Glasgow, 2010\)](#)

周波数干渉計

- 2つのパスの光路長を非対称(~38.4 cm)にして周波数安定化
(ファイバーの長さが違う)



X1干涉計

- Optical Benchに対するTM1の動きを測定
- 光検出器はQPDなので変位と角度揺れの3自由度

G. Heinzl+, [CQG 20, S153 \(2003\)](#)

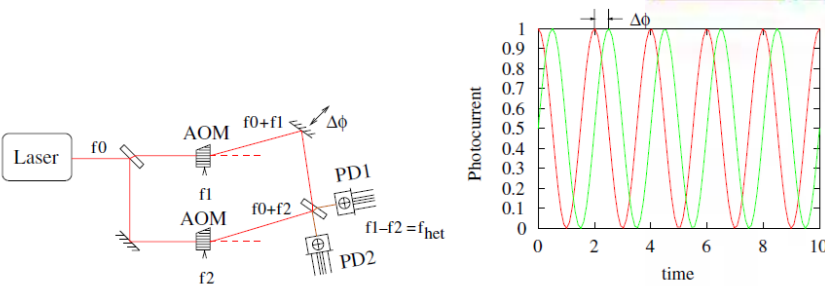
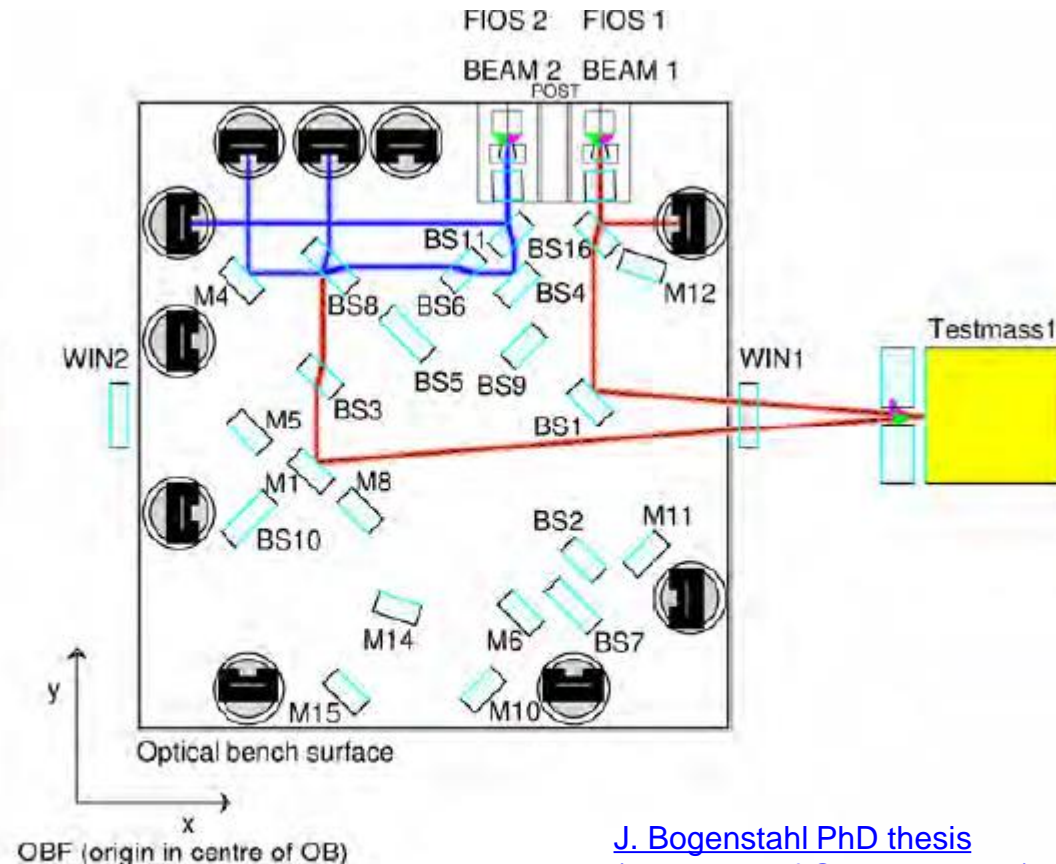


Figure 3. Heterodyne Mach-Zehnder interferometer: schematic (left) and typical photodiode signal (right).



[J. Bogenstahl PhD thesis \(University of Glasgow, 2010\)](#)

component at the heterodyne frequency f_{het} . The time dependence of the heterodyne signal is given by

$$\cos\left(2\pi f_{\text{het}} t - \frac{2\pi l}{\lambda}\right) = \cos(2\pi f_{\text{het}} t - \varphi),$$

X12干涉計

- TM1とTM2の間隔(376 mm)の変動を測定
- 相対変位と相対角度揺れの3自由度

G. Heinzl+, [CQG 20, S153 \(2003\)](#)

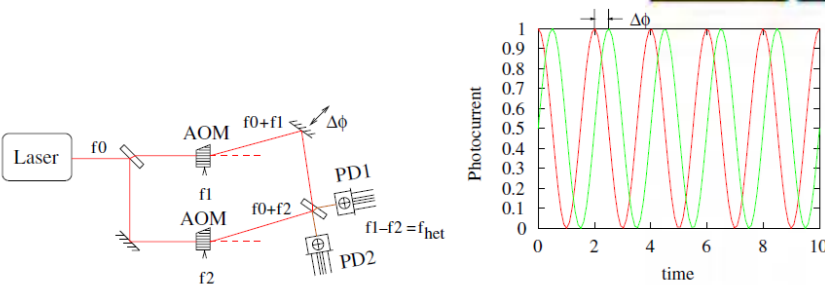
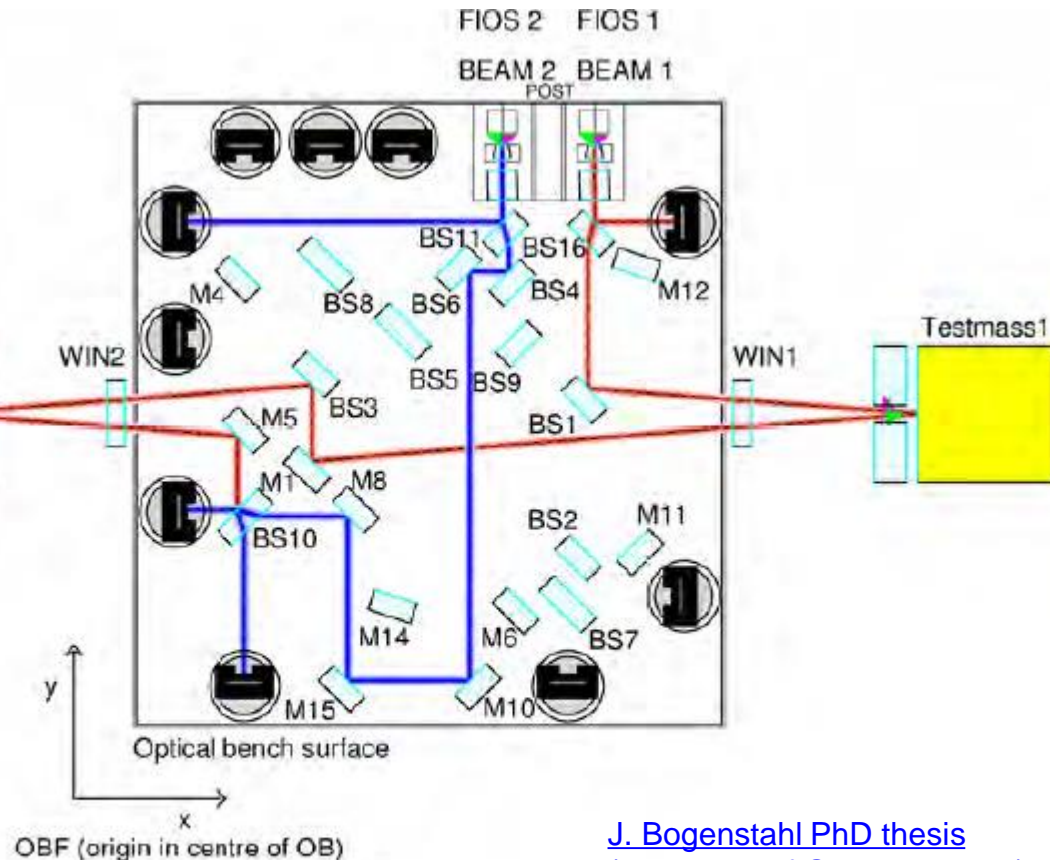


Figure 3. Heterodyne Mach-Zehnder interferometer: schematic (left) and typical photodiode signal (right).

component at the heterodyne frequency f_{het} . The time dependence of the heterodyne signal is given by

$$\cos\left(2\pi f_{het} t - \frac{2\pi l}{\lambda}\right) = \cos(2\pi f_{het} t - \varphi),$$

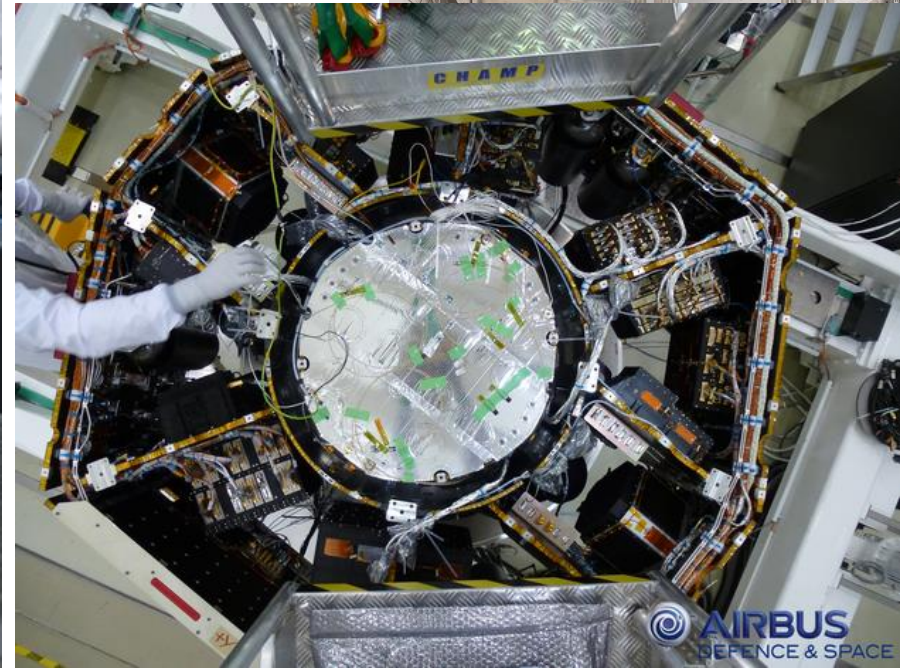
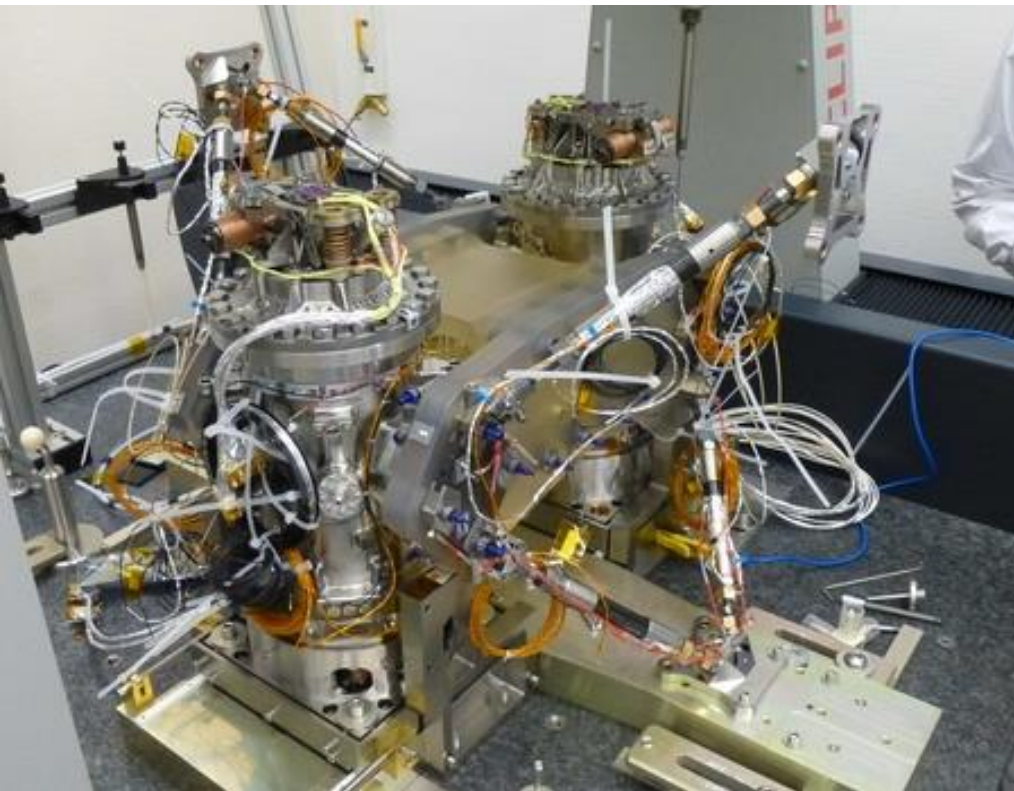


[J. Bogenstahl PhD thesis \(University of Glasgow, 2010\)](#)

LPFの中身

- LTP: LISA Technology Package
が中心部品

<http://sci.esa.int/lisa-pathfinder/56864-lisa-pathfinder-being-integrated-to-the-vega-launchers-payload-adaptor/>

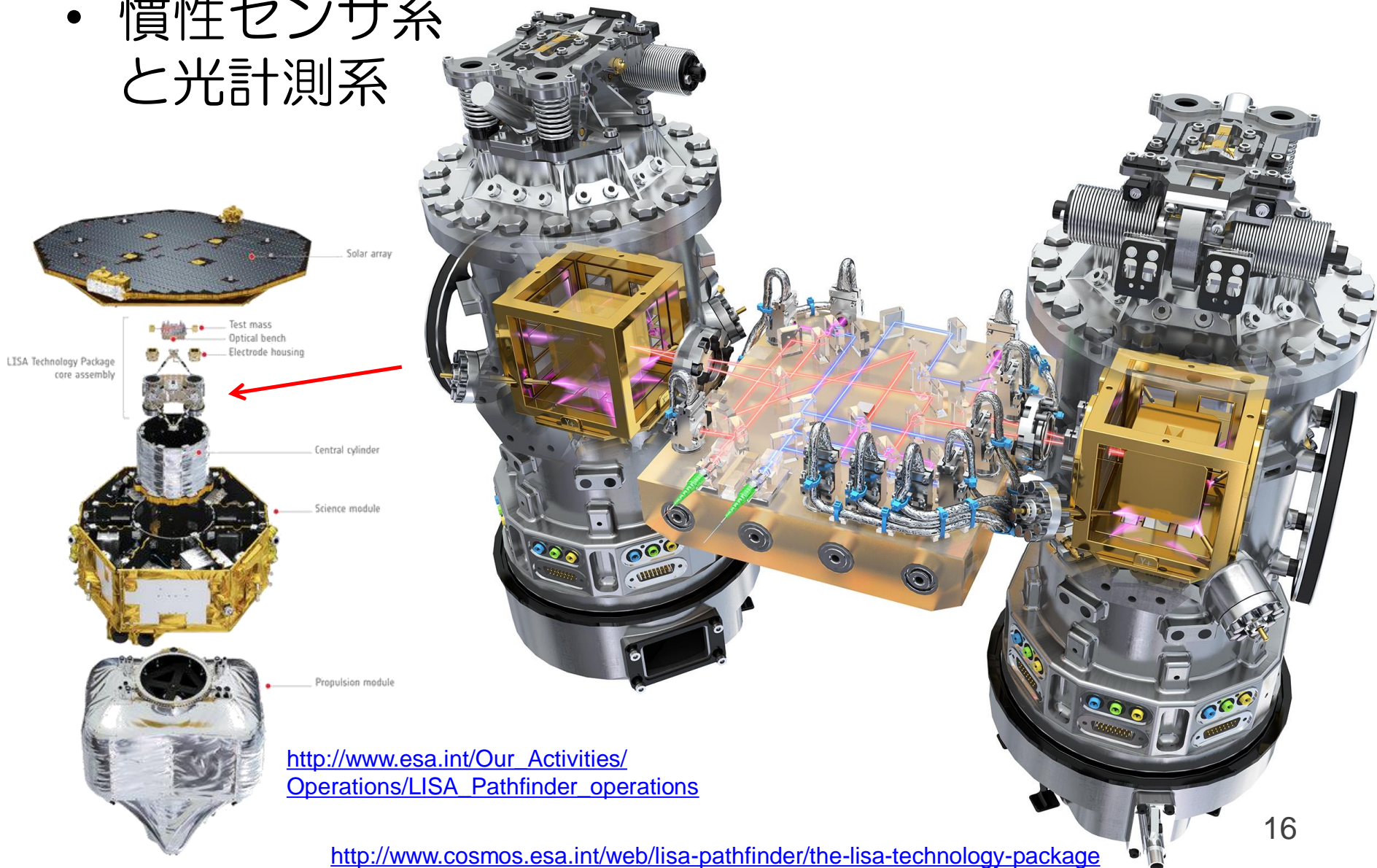


<http://sci.esa.int/lisa-pathfinder/55634-ltp-core-assembly-of-the-lisa-technology-package/>

<http://sci.esa.int/lisa-pathfinder/56025-lisa-technology-package-core-assembly-integration/>

LISA Technology Package

- 慣性センサ系
と光計測系

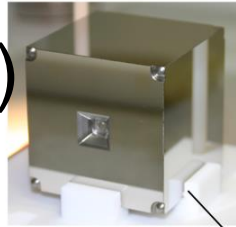


http://www.esa.int/Our_Activities/Operations/LISA_Pathfinder_operations

<http://www.cosmos.esa.int/web/lisa-pathfinder/the-lisa-technology-package>

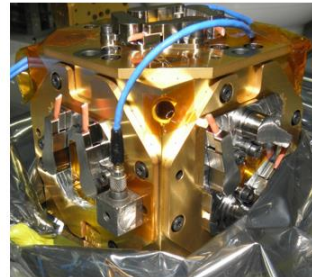
慣性センサ系

- TM(Au-Pt合金)
と極板のついでハウジング



Test Mass

静電センサ/アクチュエータ
静電場遮蔽
TM-極板間隔:
2.9-4 mm



Electrode Housing

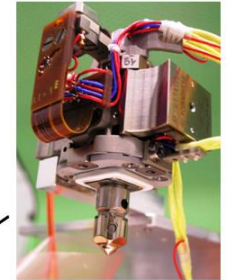
- クランプ・
リリース

機構 (打ち上げが
長年延期された要因)

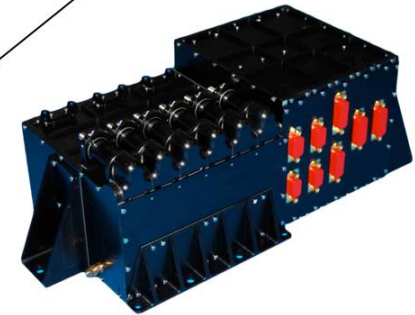
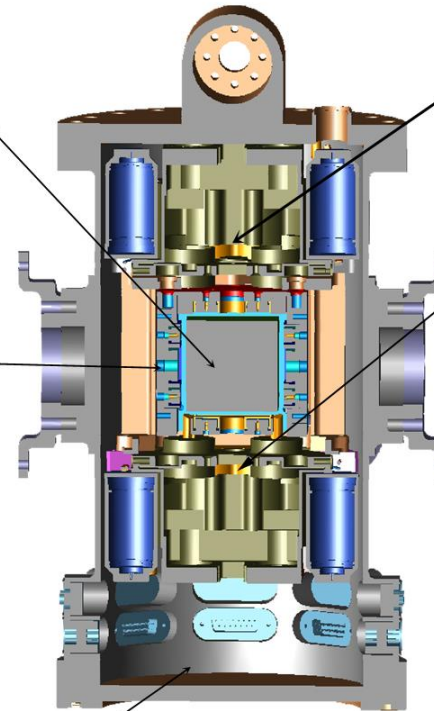
- UV帯電除去
(TMとハウ
ジング両方)



Vacuum Chamber



Grabbing, Position and
Release Mechanism



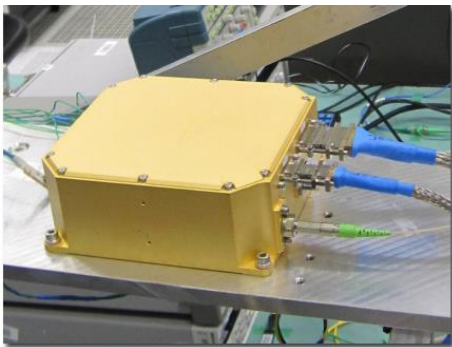
UV Light Unit



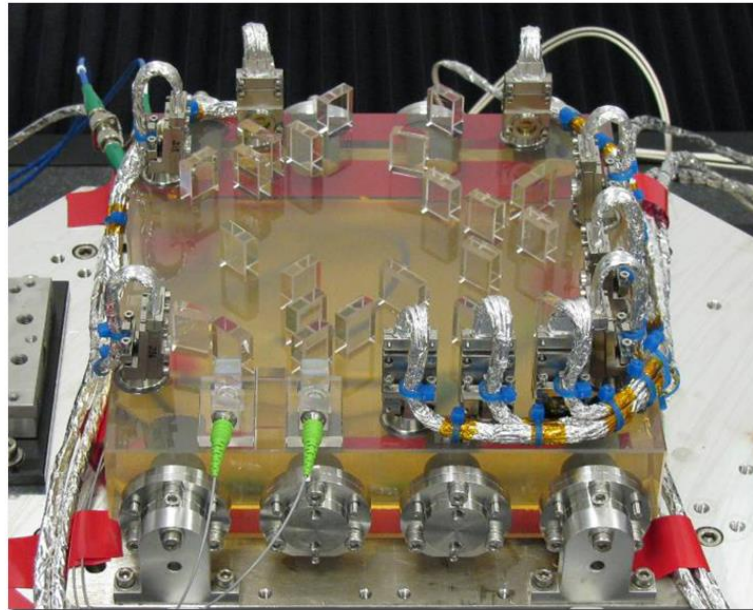
Front End Electronics

光計測系

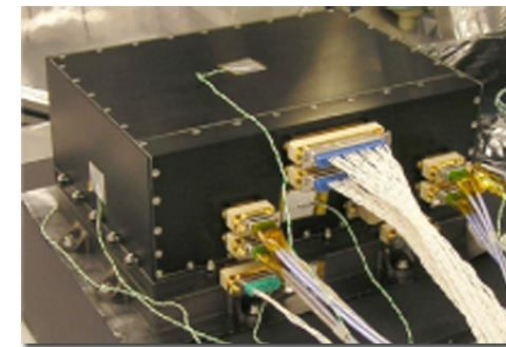
- 35 mW NPR0レーザー、強度/位相変調系(AOMで強度安定化(?)/周波数安定化)、Optical Bench、ビート周波数の位相測定器(0.2 urad/rtHz & レンジ >100 μm なのでヘテロダイン干渉計)



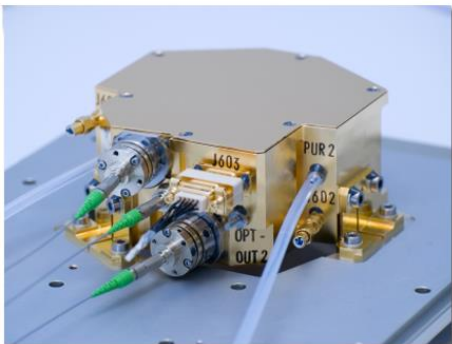
**Reference Laser Unit
(Tesat)**



**Optical Bench Interferometer
(University of Glasgow)**



**Phasemeter
(University of Birmingham)**



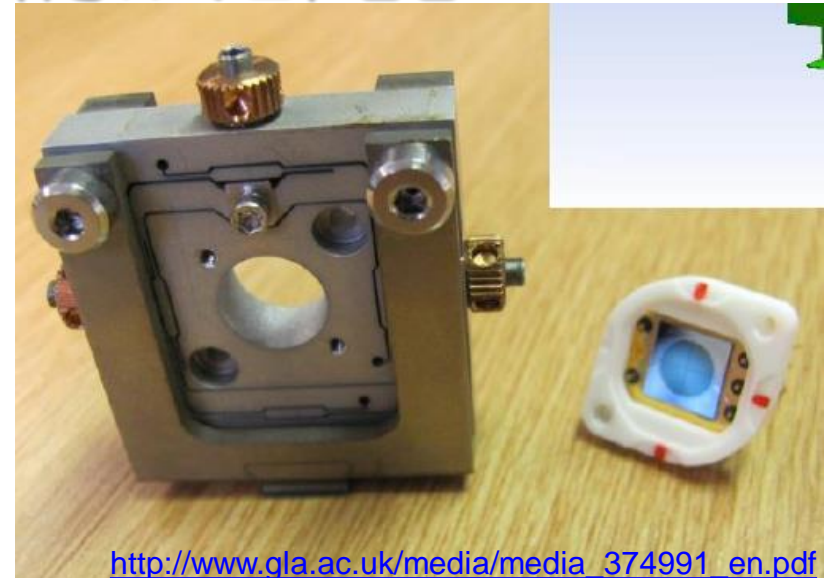
**Laser Modulator
(APC/RUAG)**



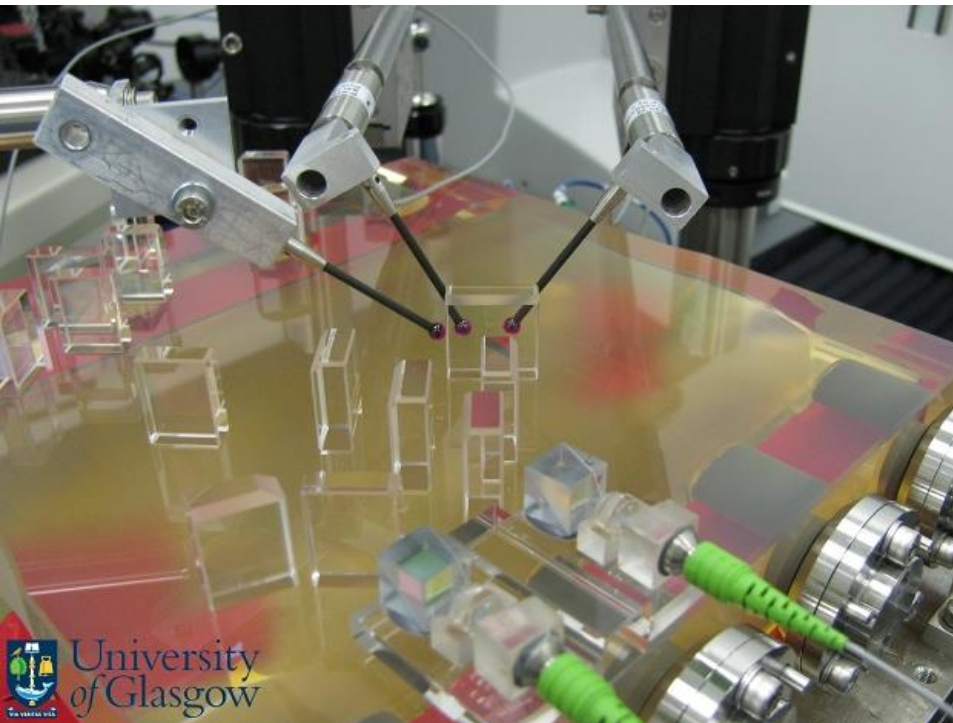
**Data Management Unit
(IEEC/NTE)**

Optical Bench構成部品

- 光検出器はQPD(InGaAS)でアライメントもモニタ



http://www.gla.ac.uk/media/media_374991_en.pdf



[J. Bogenstahl PhD thesis \(University of Glasgow, 2010\)](#)

Figure 5.1: Photograph of the fibre injector qualification model pair bonded onto the post on the prototype LTP optical bench.

穀山さんphasemeterとの比較

- LPF phasemeter: 0.2 urad/rtHz @ 0.1 Hz
(ヘテロダイン信号は1 kHz)
- 穀山さんphasemeter: 0.05 urad/rtHz @ 0.1 Hz
(使った信号は80 kHz)

W. Kokuyama+, [arXiv:1602.03701](https://arxiv.org/abs/1602.03701)

Simple digital phase-measuring algorithm for low-noise heterodyne interferometry

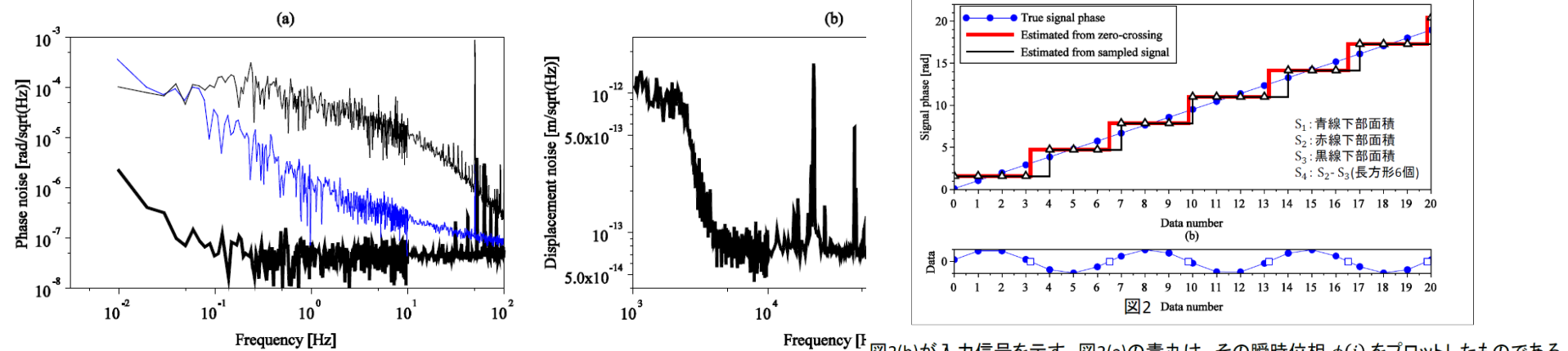
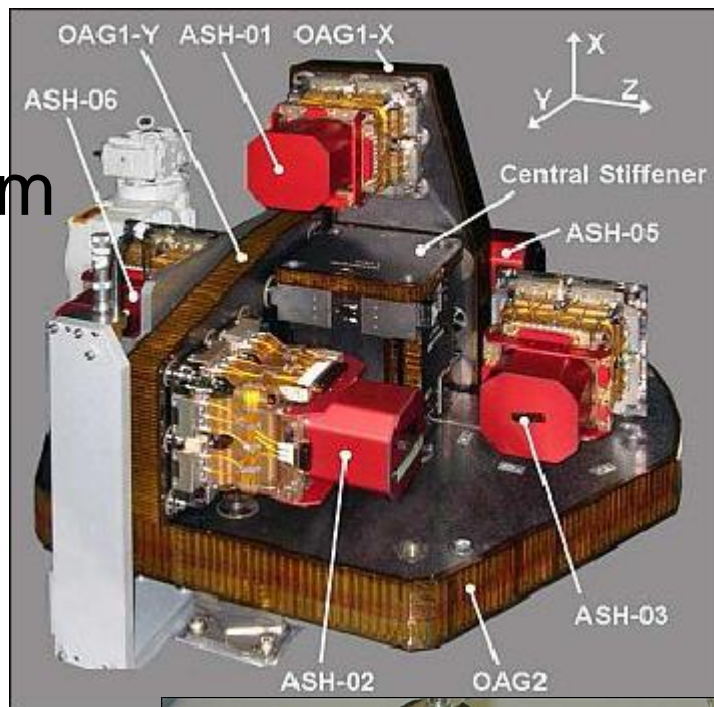


図2(b)が入力信号を示す。図2(a)の青丸は、その瞬時位相 $\phi(i)$ をプロットしたものである。このとき、(1)式の和演算は、図2 (a)青丸の下部の面積 S_1 を求めることに相当する。

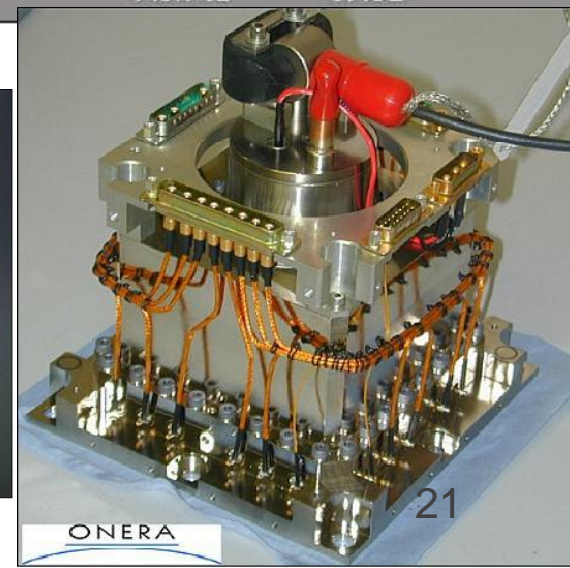
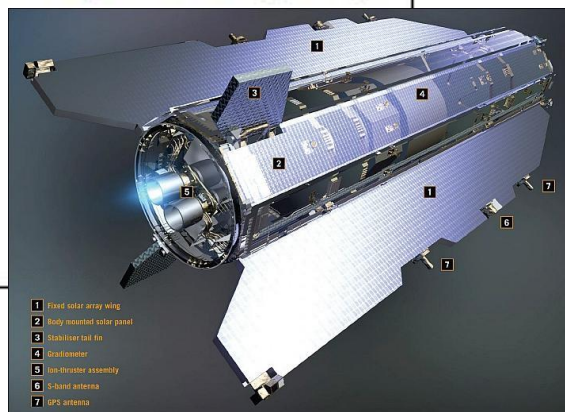
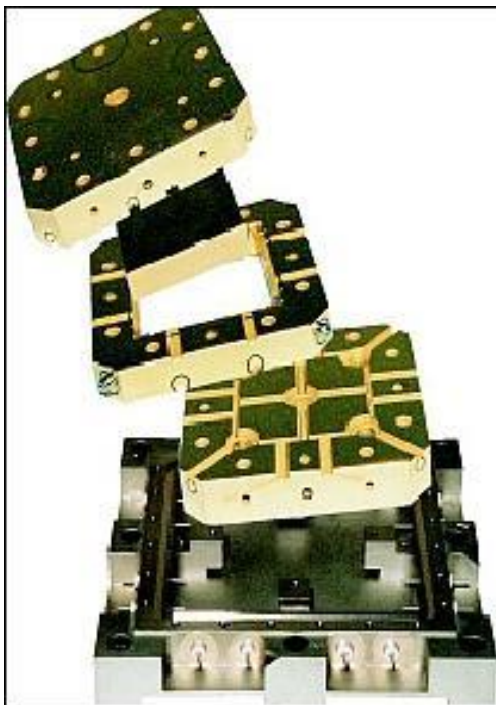
Fig. 4. (a) Results for the test with electronics. The thick line shows the result for the proposed algorithm. The thin black line shows the noise level with the lock-in amplifier and a 30 m delay line. The thin blue line shows for the result with the lock-in amplifier and an artificial phase delay implemented with a low-pass filter. (b) Results for the test with laser Doppler vibrometer.

GOCEの加速度計

- 3軸にペアの加速度計
- 320 gのTMと極板の間隔0.3 mm
- Au細線で帯電除去



- Pt-Rh proof mass of 4 x 4 x 1 cm and 320 g mass
- Accelerometer cage made of ULE ceramics with gold electrodes for 6 DOF control
- Sole plate in INVAR
- 8 electrode pairs per sensitive element (for redundancy reasons)
- Proof mass grounded by a 25 mm long and 5 μm "thick" gold wire



PRLの次のページの論文

- A. Sesana, PRL 116, 231102 (2016)
Prospects for Multiband Gravitational-Wave Astronomy after GW150914
- eLISAを使えばaLIGOで受かるBHBを先に検出可能

PRL 116, 231102 (2016)

PHYSICAL REVIEW LETTERS

week ending
10 JUNE 2016



Prospects for Multiband Gravitational-Wave Astronomy after GW150914

Alberto Sesana

School of Physics and Astronomy, University of Birmingham, Edgbaston, Birmingham B15 2TT, United Kingdom

(Received 21 February 2016; revised manuscript received 8 April 2016; published 8 June 2016)

The black hole binary (BHB) coalescence rates inferred from the Advanced LIGO detection of GW150914 imply an unexpectedly loud gravitational-wave (GW) sky at millihertz frequencies accessible to the Evolved Laser Interferometer Space Antenna (eLISA), with several outstanding consequences. First, up to thousands of BHBs will be individually resolvable by eLISA; second, millions of nonresolvable BHBs will build a confusion noise detectable with a signal-to-noise ratio of a few to hundreds; third—and perhaps most importantly—up to hundreds of BHBs individually resolvable by eLISA will coalesce in the Advanced LIGO band within 10 y. eLISA observations will tell Advanced LIGO and all electromagnetic probes weeks in advance when and where these BHB coalescences will occur, with uncertainties of <10 s and <1 deg². This will allow the prepointing of telescopes to realize coincident GW and multiwavelength electromagnetic observations of BHB mergers. Time coincidence is critical, because a prompt emission associated to a BHB merger will likely have a duration comparable to the dynamical time scale of the systems and is possible only with low-frequency GW alerts.

複数帯域での観測

- eLISAで検出してから10年以内にaLIGOで検出
 - eLISAの設計を再考すべき
 - 規模縮小はこのような科学的成果を失う
- 3本目の腕
最低2e6 km

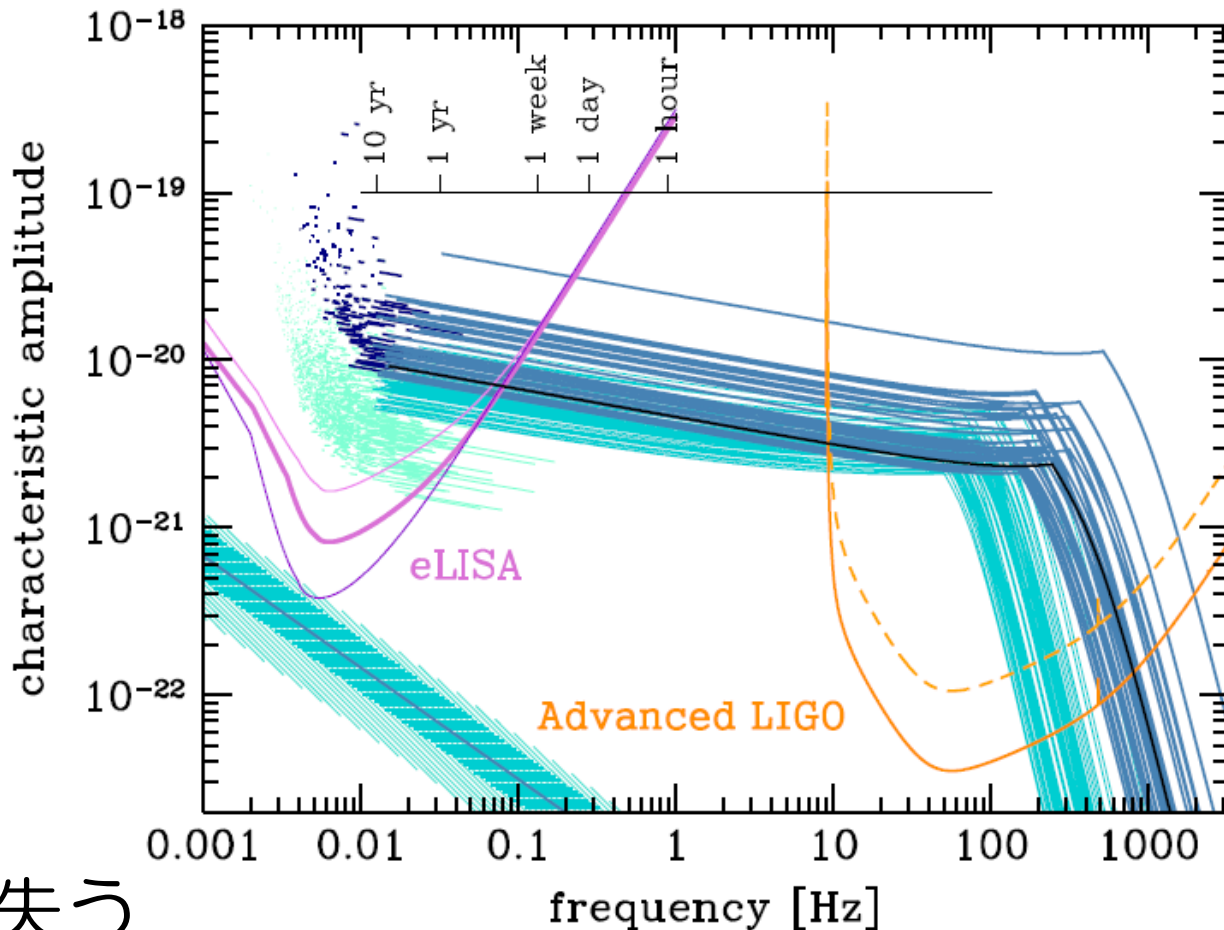


FIG. 1. The multiband GW astronomy concept. The violet lines are the total sensitivity curves (assuming two Michelson) of three eLISA configurations; from top to bottom, N2A1, N2A2, and N2A5 (from Ref. [11]). The orange lines are the current (dashed) and design (solid) Advanced LIGO sensitivity curves. The line

まとめ

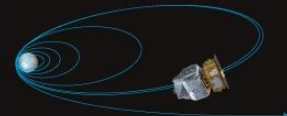
→ INVESTIGATING GRAVITY

- 極めて順調
- カッコいい

PRECISION LAB IN SPACE

LISA Pathfinder aims to test whether an intricate experiment consisting of two metal cubes in freefall, isolated from all forces except gravity, can operate in space.

When Pathfinder launches, clamps pin the cubes — which are buried at the heart of the craft — tightly to their housing so that they don't jostle and damage either themselves or other instruments.



Two hours after launch, Pathfinder separates from the launcher and begins to make increasingly elongated ellipses.

Once craft is stable, clamps release the cubes extremely gently; retractable devices position each one exactly at the centre of its housing at a speed of fewer than 5 micrometres per second. (See below).

Around 55 days into the mission, craft arrives in orbit around L-1.

51 days after launch, Pathfinder separates from thrusters.

Nine days after launch, Pathfinder makes final a burn, propelling it towards its destination — the stable point L-1, 1.5 million kilometres from Earth.

<http://www.nature.com/news/freefall-space-cubes-are-test-for-gravitational-wave-spotter-1.18806>

- 1998年に最初の提案、
- 2000年に採択、
- 当初は2006年打ち上げ予定だった

1589 GALILEO GALILEI
The acceleration of falling bodies is independent of their mass and composition

1687 ISAAC NEWTON
Universal law of gravity: the gravitational force between two bodies is directly proportional to their mass and inversely proportional to the square of their distance

1798 HENRY CAVENDISH
Torsion balance experiment to measure gravity in the laboratory. The results were later used to estimate the gravitational constant.

1915 ALBERT EINSTEIN
General theory of relativity: gravity as the interaction between massive bodies and the structure of spacetime

1919 ARTHUR EDDINGTON
First measurement, during a solar eclipse, of the deflection of light from background stars caused by the Sun, matching the amount predicted by general relativity.

1959 R. POUND & G. A. REBKA
First measurement of gravitational redshift, the frequency shift of light as it travels through the gravitational field of Earth, as predicted by general relativity.

1974 R. HULSE & J. TAYLOR
Discovery of the first pulsar in a binary system. After four years, Taylor and collaborators observed a subtle speed-up of the system: the first, indirect detection of gravitational waves.

2004-2005 GRAVITY PROBE B
Confirmation of two predictions from general relativity: the curvature of spacetime around Earth, and the 'dragging' of spacetime by Earth's rotation.

2016 ADVANCED LIGO
First direct detection of gravitational waves emitted by a pair of merging black holes.

LISA PATHFINDER
Testing technology for space-based observation of gravitational waves.